NATIONAL ADVISORY COMMITTEE FOR AERONAUTICS

TECHNICAL NOTE

No. 1548

THE DAMPING DUE TO ROLL OF TRIANGULAR, TRAPEZOIDAL, AND RELATED PLAN FORMS IN SUPERSONIC FLOW

By Arthur L. Jones and Alberta Alksne

Ames Aeronautical Laboratory
Moffett Field, Calif.

Washington
March 1948

NATIONAL ADVISORY COMMITTEE FOR AERONAUTICS

TECHNICAL NOTE NO. 1548

THE DAMPING DUE TO ROLL OF TRIANGULAR, TRAPEZOIDAL, AND RELATED PLAN FORMS IN SUPERSONIC FLOW

By Arthur L. Jones and Alberta Alksne

SUMMARY

Within the limitations of linearized potential theory for supersonic flow, solutions have been obtained for the damping in roll of triangular, trapezoidal, rectangular, and two swept-back plan forms.

The results indicate that as the aspect ratio is increased the limiting value of the damping in roll for trapezoidal (with a finite, fixed rake angle) and rectangular plan forms is equal to the value for two-dimensional flow which is twice the limiting value for triangular plan forms. For the swept-back plan forms having the Mach cone and leading edge coincident or very nearly coincident, the damping in roll even exceeded the value for two-dimensional flow.

In addition, an investigation of the effect of reversal of the plan-form position relative to the stream direction was made for the majority of the plan forms considered and the results show that this reversal had no effect on the value of the damping-in-roll stability derivative.

INTRODUCTION

There are a number of methods available for determining supersonic-flow load distributions on lifting surfaces by means of linearized potential theory. Application of any of these methods varies in detail and no individual method can be considered as being best suited for use in obtaining solutions for arbitrary Mach-cone plan-form configurations.

The relatively simple problem of determining the induced flow field and the surface shape to support an arbitrarily prescribed load distribution always can be solved using doublet distributions and a surface integration. This procedure provides an explicit expression of the doublet sheet potential. (For a detailed description see reference 1.) On the other hand, if the loading over a wing is to be determined from a knowledge of the downwash distribution required to make the streamlines conform to the shape of

the lifting surface, the doublet distribution and surface integration method again can be applied directly, provided the wing has so-called supersonic leading edges, trailing edges, and tips.[1] When subsonic edges or tips are considered, however, the mathematical development involves the solution of an integral equation in order to get results comparable to those obtained by the relatively simple surface integration used for wings with supersonic edges. The solution of an integral equation is generally a rather long and tedious process and can be circumvented for certain plan forms with subsonic leading edges or tips by a method presented in reference 2.

In this investigation to determine the linearized-potential-theory load distribution due to roll, only the surface integral methods of references 1 and 2 have been used. Other methods that have been applied successfully to obtain angle-of-attack loadings, such as the conical flow and the doublet-line methods, are also applicable.

The plan forms considered in this investigation are the following: (1) triangular with subsonic leading edges and with supersonic leading edges; (2) trapezoidal with all possible combinations of raked in, raked out, subsonic or supersonic tips (fig. 1); (3) rectangular; and (4) two swept-back plan forms developed from the triangular wings (fig. 2). Moreover, all but the swept-back plan forms and the triangular plan form with subsonic leading edges were analyzed with the stream direction reversed so that the leading edges were interchanged with the trailing edges.

The load distributions due to rolling obtained for the wings investigated were subsequently integrated to determine the rolling moment and the damping-in-roll stability derivatives. All results have been presented in stability-derivative form.

SYMBOLS AND COEFFICIENTS

x,y,z	Cartesian coordinates
u	perturbation velocity along the positive X-axis
w	perturbation velocity parallel to Z-axis (positive downward)

[1]A supersonic edge is an edge for which the angle of inclination from the plane of symmetry is greater than the Mach cone angle. The inverse of this relationship defines a subsonic edge.

V	free-stream velocity
b	span of wing measured normal to plane of symmetry
c_r	root chord of wing
l	over-all length of swept-back wing (See fig. 2)
S	area of wing
A	aspect ratio $\left(\frac{b^2}{S}\right)$
ρ	density in the free stream
q	free-stream dynamic pressure $(\frac{1}{2}\rho V^2)$
ΔP	pressure differential across wing surface, positive upward
L	rolling moment about X-axis
C_l	rolling-moment coefficient $\left(\frac{L}{qSb}\right)$
p	rate of roll, radians per second
C_{l_p}	damping-in-roll stability derivative $\left(\frac{\partial C_l}{\partial(pb/2V)}\right)$
M	free-stream Mach number
β	$\sqrt{M^2-1}$
μ	Mach angle $\left(\text{arc tan } \frac{1}{\beta}\right)$
δ	tip rake angle measured from line parallel to plane of symmetry in plane of wing
m	tangent of δ
θ	$\frac{\tan \delta}{\tan \mu}$
E	complete eliptic integral of the second kind with modulus $\sqrt{1-\theta^2}$
K	complete elliptic integral of the first kind with modulus $\sqrt{1-\theta^2}$
Φ	perturbation velocity potential

METHOD

The thin-airfoil-theory boundary condition for a rolling wing is a linear spanwise variation of angle of attack which corresponds to a linear spanwise distribution of the vertical induced velocity w. The problem, therefore, is to find the load distribution that will satisfy this condition within the wing boundaries and conform in all other respects to a proper solution of the linearized differential equation for supersonic flow. A detailed development and discussion of the surface integral method for obtaining the load distribution for a rolling wing can be found in reference 1. The presentation of the method in this report is merely an outline of the operations involved in obtaining the load distribution from the known boundary conditions.

The loading at any point is proportional to the perturbation velocity u parallel to the longitudinal axis of the wing (the X-axis in figs. 1 and 2). The following simple relationships from linearized potential theory

$$u = \frac{\partial \Phi}{\partial x} = \frac{\partial}{\partial x}\int_{\text{cone}}^{z} w \, dz \tag{1}$$

$$\frac{\Delta P}{q} = \frac{4u}{V} \tag{2}$$

can be used to obtain u and subsequently the load distribution in terms of $\frac{\Delta P}{q}$ once the general expression for the vertical induced velocity w required in equation (1) is known.

To convert the load distribution into rolling moment about the X-axis the following integration must be performed:

$$\frac{L}{q} = \iint_{\substack{\text{wing} \\ \text{plan form}}} \frac{\Delta P}{q} \, y \, dy \, dx$$

The stability derivative coefficient C_{l_p} is then

$$C_{l_p} = \frac{\partial C_l}{\partial\left(\frac{pb}{2V}\right)} = \frac{2VL}{qSb^2p}$$

The general expression for w must be known in the region directly above the wing extending from the wing to the Mach cone envelope. The procedures for obtaining this expression are divided into the two following categories for discussion.

Supersonic Leading Edges and Tips

An application of Green's theorem, discussed in reference 1, provides the means for determining a general expression for w if w is specified in the plane of the wing over the area bounded by the envelope of the Mach forecones stemming from the trailing edges. The means used amounts to an integration over a doublet sheet for which the strength is proportional to the specified values of w on the X-Y plane. For the supersonic-edged plan forms, therefore, the loading solution can be obtained readily, since w is equal to zero in the bounded area of the X-Y plane except on the wing itself where w is equal to the prescribed boundary-condition value.

Subsonic Leading Edges or Tips

If the plan form has a subsonic leading edge or tips, the air can be disturbed in the region between the foremost Mach cone and the wing surface. In this region, therefore, the specification of w on the X-Y plane requires in general that an integral equation must be solved to obtain the general expression for w. Reference 2, however, provides an alternative procedure for certain types of subsonic leading-edge or tip plan forms whereby the solution of an integral equation may be avoided. The solutions for these plan forms then are obtained by a process of integration similar to the procedure used for plan forms with supersonic tips and leading edges.

DISCUSSION OF RESULTS

The stability-derivative results are divided into the triangular plan form, the trapezoidal and rectangular plan form, and the

swept-back plan-form categories for discussion. Expressions for the stability-derivative coefficients are given. Curves showing the variation of these coefficients with aspect ratio are presented in figures 3, 4, and 5. Expressions for the loading function $\Delta P/q$ are given in Appendix A.

Triangular Plan Forms

The expression for C_{l_p} for the triangular plan form[2] with supersonic leading edges is

$$\beta C_{l_p} = -\frac{1}{3}$$

and for the triangular wing with subsonic leading edges it is

$$\beta C_{l_p} = \frac{-\pi\theta}{4\left(\frac{2-\theta^2}{1-\theta^2}E - \frac{\theta^2}{1-\theta^2}K\right)}$$

where E is the complete elliptic integral of the second kind with modulus $\sqrt{1-\theta^2}$, K is the complete elliptic integral of the first kind with modulus $\sqrt{1-\theta^2}$, and θ is a parameter that indicates the relative positions of the Mach cone and leading edge. For the subsonic leading-edge plan forms the value of θ is less than 1 and the leading edge is swept behind the Mach cone. The variation of βC_{l_p} with the aspect ratio parameter βA is presented in figure 3 for both types of triangular plan forms.

Trapezoidal and Rectangular Plan Forms

There are two general types of trapezoidal plan forms, defined by having the tip either raked in or raked out from the leading edge. The tip in either case may be classified as subsonic or supersonic depending on whether the Mach-cone angle is greater or less than the rake angle. Thus there are four basic Mach-cone plan-form

[2]Triangular plan forms with the point forward will be referred to as "triangular plan forms" in contrast to the term "inverted triangular plan forms" which will be used in reference to base forward triangles.

configurations. For three of these configurations the possibility of the overlapping of the Mach cones from the tips provides a secondary configuration for which it is possible to predict the loading distribution and the damping due to roll. All the trapezoidal plan forms considered are shown in figure 1.

The expression for βC_{l_p} for the trapezoidal plan forms with supersonic tips $(\theta \geq 1)$

$$\beta C_{l_p} = -\frac{2}{3}\left(1 - \frac{2\theta}{\beta A}\right)$$

was found to apply regardless of whether the tip was raked in, as on plan form a, or raked out, as on plan form b. Since for a given θ and a given span the plan forms a and b are effectively the same plan form with the stream direction reversed, it is evident that C_{l_p} is independent of the direction of the stream, provided the stream remains parallel to the plane of symmetry of the plan form. The same conclusion applies to the subsonic-tipped trapezoidal and rectangular plan forms $(\theta < 1)$ and the expression for βC_{l_p} for this type is

$$\beta C_{l_p} = \frac{-\beta A}{12}\frac{c_r}{\beta b}\left[8 - \frac{12c_r}{\beta b}(1 + \theta) + \frac{4c_r^2}{\beta^2 b^2}(1 + 4\theta + 3\theta^2)\right.$$

$$\left. + \frac{c_r^3}{\beta^3 b^3}(1 - 3\theta - 9\theta^2 - 5\theta^3)\right]$$

This property of reversibility appears to be rather remarkable in view of the fact that the load distribution on a given plan form is changed markedly by reversing the stream direction. This result also is a direct analogue to von Kármán's independence theorem (reference 3) for drag and, although the drag theorem was developed analytically to apply to all plan forms, the independence of the lift and roll characteristics as yet merely has been indicated by calculation on a limited number of plan forms.

It is obvious that the trapezoidal plan form can be reduced in span till either a triangular or an inverted triangular plan form is obtained. Thus it was possible to check on the reversibility property of the supersonic-leading-edge triangles quite readily. It was not possible in the present investigation, however, to reduce the subsonic-tipped trapezoids to triangles corresponding to

inverted triangular wings in order to obtain a check on the independence theorem for these plan forms. As βA becomes less than $(1 + \theta)^2$ the Mach cone from one tip is reflected off the other tip and the load distribution behind these reflected Mach lines is not readily determined. From figure 3 it is apparent that, for values of βA less than $(1 + \theta)^2$, the variation of βC_{l_p} with βA must reduce in slope as the trapezoid reduces to a triangle $(\beta A = 4\theta)$ in order to yield the value of βC_{l_p} corresponding to the value of βC_{l_p} for the triangular plan form.

It can be seen in figure 3 that as the aspect ratio increases the values of βC_{l_p} for the trapezoidal and rectangular plan forms approach the value for two-dimensional flow $-\frac{2}{3}$; whereas the triangular plan forms reach a value of $-\frac{1}{3}$ when the aspect ratio parameter βA becomes equal to or greater than 4. By letting the tangent of the rake angle approach infinity as the span approaches infinity, the supersonic-tipped trapezoidal plan forms can be made to approach the configuration of an inverted triangular plan form. Since for a triangular plan form

$$A = 4m$$

the limiting value of βC_{l_p} for this case becomes (using the expression for the supersonic-tipped trapezoidal plan forms)

$$\beta C_{l_p} = -\frac{2}{3}\left(1 - \frac{2\theta}{\beta A}\right)$$

$$= -\frac{2}{3}\left(1 - \frac{2\beta m}{\beta 4m}\right)$$

$$\beta C_{l_p} = -\frac{2}{3}\left(1 - \frac{1}{2}\right) = -\frac{1}{3}$$

and thus checks with the value for the triangular plan form with supersonic edges.

Swept-Back Plan Forms

The two swept-back plan forms shown in figure 2 are easily developed from the triangular wings of supersonic and subsonic leading edges by cutting out a small triangular area from the rear of the triangular plan forms. Other swept-back plan-form configurations

are also amenable to calculation but only the results for the two plan forms selected are included in this report for purposes of comparison. The expression for the damping in roll of the swept-back plan form with subsonic leading edges is

$$\beta C_{l_p} = \frac{\beta(L_1-L_2)}{qSb}\frac{2V}{pb} = \frac{\beta(L_1-L_2)2V}{\frac{1}{\beta}\left[l\left(\frac{\beta b}{2}+2c_r\right)-l^2-c_r{}^2\right]qpb^2}$$

where L_1 is the rolling moment for the triangular wing as a whole and L_2 is the rolling moment of the small triangle cut out to provide a swept-back plan form. The expressions for L_1 and L_2 are given in Appendix B.

For the swept-back plan form with supersonic leading edges the damping-in-roll coefficient is

$$\beta C_{l_p} = \frac{\beta(L_3-L_4)}{qSb}\frac{2V}{pb} = \frac{\beta(L_3-L_4)2V}{m\left[l\left(\frac{b}{2m}+2c_r\right)-l^2-c_r{}^2\right]qpb^2}$$

where L_3 is the rolling moment for the triangular wing as a whole and L_4 is the rolling moment of the small triangle cut out to provide a swept-back plan form. The expressions for L_3 and L_4 are given in Appendix B.

From figure 5 it can be seen that both of these swept-back plan forms provided more damping in roll than their related triangular plan forms of the same span and Mach-cone leading-edge configuration. This result was anticipated, since the load distributions for the triangular plan forms in roll reveal that the magnitude of the load increases as the leading edges are approached. At values of θ in the immediate vicinity of 1, the swept-back plan forms provide greater damping in roll than the trapezoidal or rectangular plan forms for comparable values of βA. Moreover, even the value of βC_{l_p} for two-dimensional flow $-\frac{2}{3}$ is exceeded in magnitude at βA's of 10 or higher by the swept-back plan forms of the type shown on which the Mach cone and leading edge are very nearly coincident (θ very nearly equal to 1).

CONCLUDING REMARKS

The results of this investigation based on linearized potential theory indicate that for values of βA greater than 4 the trapezoidal and rectangular plan forms provide values of $-\beta C_{l_p}$ greater than the limiting value $\frac{1}{3}$ for the triangular plan forms. The limiting value of $-\beta C_{l_p}$ for the rectangular and trapezoidal (with a finite, fixed rake angle) plan forms is $\frac{2}{3}$ which corresponds to the value for a constant-chord plan form of infinite span. The value of $\frac{1}{3}$ for $-\beta C_{l_p}$ is also exceeded by some of the swept-back plan forms. The swept-back plan forms investigated, moreover, showed that for configurations on which the Mach cone and the leading edge are very nearly coincident the value of $-\beta C_{l_p}$ for two-dimensional flow $\frac{2}{3}$ is exceeded.

All but the swept-back plan forms and the triangular plan form with subsonic leading edges were investigated with the leading edges and trailing edges reversed relative to the stream direction. For a given plan form at a given Mach number it was found that this reversal, which changed completely the distribution of the load, had no effect on the value of βC_{l_p}.

Ames Aeronautical Laboratory,
National Advisory Committee for Aeronautics,
Moffett Field, Calif.

APPENDIX A

The expressions for the load distribution over the triangular plan forms are as follows:

$\theta \geq 1$ (Supersonic leading edges) Region within the Mach cone

$$\frac{\Delta P}{q} = \frac{4p}{V}\left\{\left[\frac{m(\theta^2 y - mx)}{\pi(\theta^2-1)^{3/2}}\right]\sin^{-1}\left[\frac{\theta^2 y - mx}{\theta(mx-y)}\right]\right.$$

$$\left. - \left[\frac{m(\theta^2 y + mx)}{\pi(\theta^2-1)^{3/2}}\right]\sin^{-1}\left[\frac{\theta^2 y + mx}{\theta(mx+y)}\right] + \frac{m\theta^2 y}{(\theta^2-1)^{3/2}}\right\}$$

Region between Mach cone and leading edge

$$\frac{\Delta P}{q} = \frac{4pm(\theta^2 y - mx)}{V(\theta^2-1)^{3/2}}$$

$\theta < 1$ (Subsonic leading edges)

$$\frac{\Delta P}{q} = \frac{4p\, m^2 yx}{V\sqrt{m^2x^2-y^2}\left[\frac{2-\theta^2}{1-\theta^2}E - \frac{\theta^2}{1-\theta^2}K\right]}$$

The expressions for the load distributions for the trapezoidal plan forms shown in figure 1 and for the rectangular plan form are as follows:

$\theta \geq 1$

Plan form a, $\beta A \geq 4$

$$\frac{\Delta P}{q} = \frac{4py}{\beta V}$$

Plan form b, $\beta A \geq 4(\theta+1)^2/(\theta+2)$

Region 1

$$\frac{\Delta P}{q} = \frac{4py}{\beta V}$$

Region 2

$$\frac{\Delta P}{q} = \frac{4p}{V}\left\{\left[\frac{m\left(\theta^2 y - mx - \frac{b}{2} + mc_r\right)}{\pi(\theta^2-1)^{3/2}}\right] \sin^{-1}\left[\frac{\theta^2\left(y - \frac{b}{2} + mc_r\right) - mx}{\theta\left(xm - y + \frac{b}{2} - c_r\right)}\right]\right.$$

$$+ \frac{m\left(\theta^2 y - mx - \frac{b}{2} + mc_r\right)}{2(\theta^2-1)^{3/2}} - \frac{my}{\pi\theta}\sin^{-1}\left[\frac{\theta\left(y - \frac{b}{2} + mc_r\right)}{mx}\right] + \frac{my}{2\theta}$$

$$\left. + \frac{m\sqrt{m^2x^2 - \theta^2\left(y - \frac{b}{2} + mc_r\right)^2}}{\pi\,\theta^2(\theta^2-1)}\right\}$$

Region 3

$$\frac{\Delta P}{q} = \frac{4p}{V}\left[\frac{m\left(\theta^2 y - mx - \frac{b}{2} + mc_r\right)}{(\theta^2-1)^{3/2}}\right]$$

Plan form c, $4 \leq \beta A \leq 4(\theta+1)^2/(\theta+2)$

Region 1 $\frac{\Delta P}{q}$ same as for region 1 on plan form b

Region 2 $\frac{\Delta P}{q}$ same as for region 2 on plan form b

Region 3 $\frac{\Delta P}{q}$ same as for region 3 on plan form b

Region 4

$$\frac{\Delta P}{q} = \left(\frac{\Delta P}{q}\right)_2 - \left(\frac{\Delta P}{q}\right)_1 - \frac{4p}{V}\left\{\left[\frac{m(-\theta^2 y - mx - \frac{b}{2} + mc_r)}{\pi(\theta^2-1)^{3/2}}\right]\sin^{-1}\left[\frac{\theta^2(-y-\frac{b}{2}+mc_r)-mx}{\theta(xm-y+\frac{b}{2}-c_r)}\right]\right.$$

$$+ \frac{m(-\theta^2 y - mx - \frac{b}{2} + mc_r)}{2(\theta^2-1)^{3/2}} + \frac{my}{\pi\theta}\sin^{-1}\left[\frac{\theta(-y-\frac{b}{2}+mc_r)}{mx}\right] - \frac{my}{2\theta}$$

$$\left. + \frac{m\sqrt{m^2x^2-\theta^2(-y-\frac{b}{2}+mc_r)^2}}{\pi\theta^2(\theta^2-1)}\right\}$$

$\theta < 1$

Plan form d, $\beta A \geq 4/(2-\theta)$

Region 1

$$\frac{\Delta P}{q} = \frac{4py}{\beta V}$$

Region 2

$$\frac{\Delta P}{q} = \frac{4p}{\beta V}\left[\frac{y}{\pi}\cos^{-1}\frac{2\beta(y-\frac{b}{2})+x+\theta x}{x(1-\theta)} - \frac{2\sqrt{-(\beta y-\beta\frac{b}{2}+x)(\beta y-\beta\frac{b}{2}+\theta x)}}{\pi\beta(1-\theta)}\right]$$

Plan form e, $(1+\theta)^2 \leq \beta A \leq 4/(2-\theta)$

Region 1 $\frac{\Delta P}{q}$ same as for region 1 on plan form d.

Region 2 $\frac{\Delta P}{q}$ same as for region 2 on plan form d.

Region 3

$$\frac{\Delta P}{q} = \left(\frac{\Delta P}{q}\right)_2 - \left(\frac{\Delta P}{q}\right)_1 + \frac{4p}{\beta V}\left\{\frac{y}{\pi}\cos^{-1}\left[\frac{2\beta(-y-\frac{b}{2})+x+\theta x}{x(1-\theta)}\right] + \frac{2\sqrt{(\beta y+\beta\frac{b}{2}-x)(\theta x-\beta y-\beta\frac{b}{2})}}{\pi\,\beta(1-\theta)}\right\}$$

Plan form f, $\beta A \geq 4(\theta+1)^2/(\theta+2)$

Region 1

$$\frac{\Delta P}{q} = \frac{4py}{\beta V}$$

Region 2

$$\frac{\Delta P}{q} = \frac{4p}{\beta V}\left\{\frac{y}{\pi}\cos^{-1}\left[\frac{2(\beta y-\beta\frac{b}{2}+\theta c_r)+x-\theta x}{x(1+\theta)}\right]\right.$$

$$-\frac{2\sqrt{(x+\beta y-\beta\frac{b}{2}+\theta c_r)(\theta x-\beta y+\beta\frac{b}{2}-\theta c_r)}}{\pi\,\beta(1+\theta)}$$

$$\left.+\left[\frac{6\theta^2(\beta y+x)-2\theta(\beta y+x+4\theta c_r-4\beta\frac{b}{2})}{3\pi\beta(1+\theta)^2}\right]\sqrt{\frac{(x+\beta y-\beta\frac{b}{2}+\theta c_r)}{(\theta x-\beta y+\beta\frac{b}{2}-\theta c_r)}}\right\}$$

Plan form g, $(1+\theta)^2 \leq \beta A \leq 4(1+\theta)^2/(\theta+2)$

Region 1 $\frac{\Delta P}{q}$ same as for region 1 on plan form f.

Region 2 $\frac{\Delta P}{q}$ same as for region 2 on plan form f.

Region 3

$$\frac{\Delta P}{q} = \left(\frac{\Delta P}{q}\right)_2 - \left(\frac{\Delta P}{q}\right)_1 + \frac{4p}{\beta V}\left\{\frac{y}{\pi}\cos^{-1}\left[\frac{2\left(-\beta y-\beta\frac{b}{2}+\theta c_r\right)+x-\theta x}{x(1+\theta)}\right]\right.$$

$$+\frac{2\sqrt{\left(x-\beta y-\beta\frac{b}{2}+\theta c_r\right)\left(\theta x+\beta y+\beta\frac{b}{2}-\theta c_r\right)}}{\pi\beta(1+\theta)}$$

$$\left.+\left[\frac{6\theta^2(\beta y-x)+2\theta\left(x-\beta y+4\theta c_r-4\beta\frac{b}{2}\right)}{3\pi\beta(1+\theta)^2}\right]\sqrt{\frac{x-\beta y-\beta\frac{b}{2}+\theta c_r}{\theta x+\beta y+\beta\frac{b}{2}-\theta c_r}}\right\}$$

$\theta = 0$ (rectangular) $\beta A \geq 1$

$\frac{\Delta P}{q}$ same as for trapezoidal plan form e with $\theta = 0$.

APPENDIX B

The expressions for the rolling moments L_1, L_2, L_3, and L_4 for the swept-back plan forms are:

$$L_1 = \frac{-pqb^4\pi}{32V\left(\frac{2-\theta^2}{1-\theta^2}E - \frac{\theta^2}{1-\theta^2}K\right)}$$

$$L_2 = \frac{-8pqm^2}{V\left(\frac{2-\theta^2}{1-\theta^2}E - \frac{\theta^2}{1-\theta^2}K\right)} \left\{ \left[\frac{c_r{}^4\theta^2(4\theta^2+1)}{8\beta^2(1-\theta^2)^{7/2}}\right] \right.$$

$$\left[\sin^{-1}\frac{c_r - l(1-\theta^2)}{c_r\theta} - \sin^{-1}\theta\right] - \frac{\sqrt{l^2\theta^2-(l-c_r)^2}}{24\beta^2(1-\theta^2)^3}$$

$$\left[3l^3 - 5l^2c_r + lc_r + c_r{}^3 - \theta^2(9l^3 - 13l^2c_r + 72c_r{}^2 + 10c_r{}^3)\right.$$

$$\left. + \theta^4(9l^3 - 11l^2c_r + 6lc_r{}^2 - 6c_r{}^3) - 3\theta^6(l^3 - l^2c_r)\right]$$

$$\left. - \frac{c_r{}^4\theta^3(2\theta^2+13)}{24\beta^2(1-\theta^2)^3} + \frac{l^4\theta^2}{8\beta^2}\sin^{-1}\left(\frac{l-c_r}{l\theta}\right)\right\}$$

$$L_3 = \frac{-2pql^4m^4}{3V\theta}$$

$$L_4 = \frac{-2pqm^4}{\pi V(\theta-1)^{3/2}} \left\{ c_r^4 \left(\left[\frac{-(3\theta^2+2)}{12(\theta^2-1)^2} - \frac{(\theta^2-2)}{12} \right] \sin^{-1} \frac{1}{\theta} + \frac{(3\theta^2+2)(\theta^2-4)}{36(\theta^2-1)^{3/2}} \right.\right.$$

$$+ \left[\frac{(\theta^2+1)(l-c_r)^3}{3c_r^3} + \frac{(l-c_r)^2}{2c_r^2} + \frac{(\theta^2-2)}{24} \right] \sin^{-1} \frac{\theta^2(l-c_r)+l}{\theta(2l-c_r)}$$

$$+ \left[- \frac{(\theta^2-1)(l-c_r)^3}{3c_r^3} + \frac{(l-c_r)^2}{2c_r^2} - \frac{(\theta^2-2)}{24} - \frac{(3\theta^2+2)}{12(\theta^2-1)^2} \right] \sin^{-1} \frac{\theta^2(l-c_r)-l}{\theta c_r}$$

$$\left. + \frac{\sqrt{l^2-\theta^2(l-c_r)^2}}{c_r} \left[- \frac{(l-c_r)^2\sqrt{\theta^2-1}}{9c_r^2} + \frac{(l-c_r)(3\theta^2+2)}{36c_r\sqrt{\theta^2-1}} - \frac{(3\theta^2+2)(\theta^2-4)}{36(\theta^2-1)^{3/2}} \right] \right)$$

$$+ l^4 \left(\left[- \frac{\theta^2(l-c_r)^3}{3l^3} - \frac{(l-c_r)^2}{2l^2} - \frac{(2\theta^2-3)}{6} \right] \sin^{-1} \frac{\theta^2(l-c_r)+l}{\theta(2l-c_r)} \right.$$

$$+ \left[\frac{\theta^2(l-c_r)^3}{3l^3} - \frac{(l-c_r)^2}{2l^2} - \frac{(2\theta^2-3)}{6} \right] \sin^{-1} \frac{\theta^2(l-c_r)-l}{\theta c_r}$$

$$+ \frac{\pi(\theta^2-1)^{3/2}}{3\theta} - \frac{(l-c_r)\sqrt{\theta^2-1}\sqrt{l^2-\theta^2(l-c_r)^2}}{3l^2}$$

$$\left. \left. - \left[\frac{2(\theta^2-1)^{3/2}}{3\theta} \right] \cos^{-1} \frac{\theta(l-c_r)}{l} \right) + \frac{(l-c_r)^4\pi\theta^2}{3} \right\}$$

REFERENCES

1. Heaslet, Max. A., and Lomax, Harvard: The Use of Source-Sink and Doublet Distributions Extended to the Solution of Arbitrary Boundary Value Problems in Supersonic Flow. NACA TN No. 1515, 1947.

2. Evvard, John C.: Distribution of Wave Drag and Lift in the Vicinity of Wing Tips at Supersonic Speeds. NACA TN No. 1382, 1947.

3. von Kármán, Theodore: Supersonic Aerodynamics--Principles and Applications. Jour. Aero. Sci. vol. 14, no. 7, July 1947.

$\theta > 1$

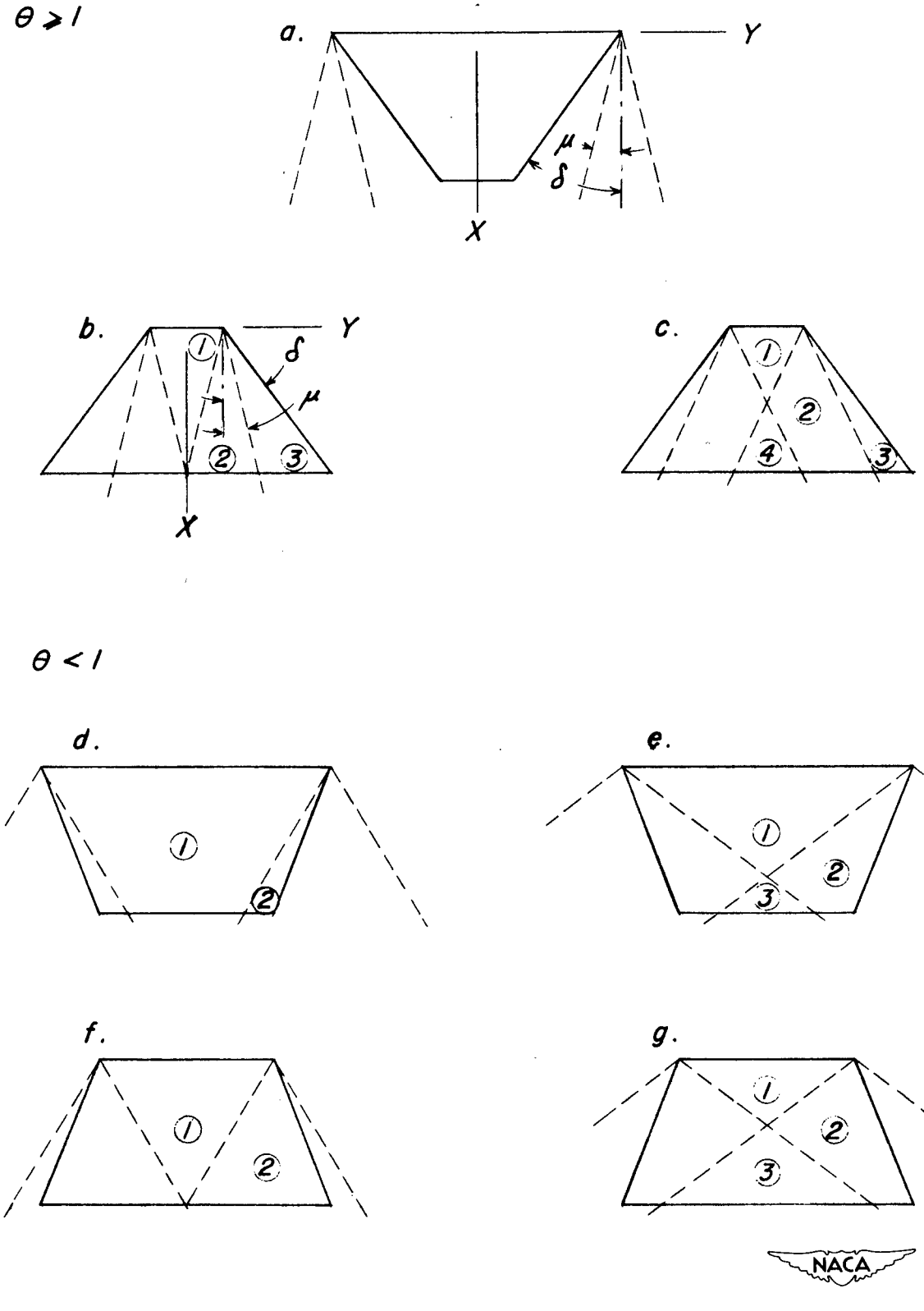

$\theta < 1$

Figure 1.- Trapezoidal planforms and Mach cone configurations investigated.

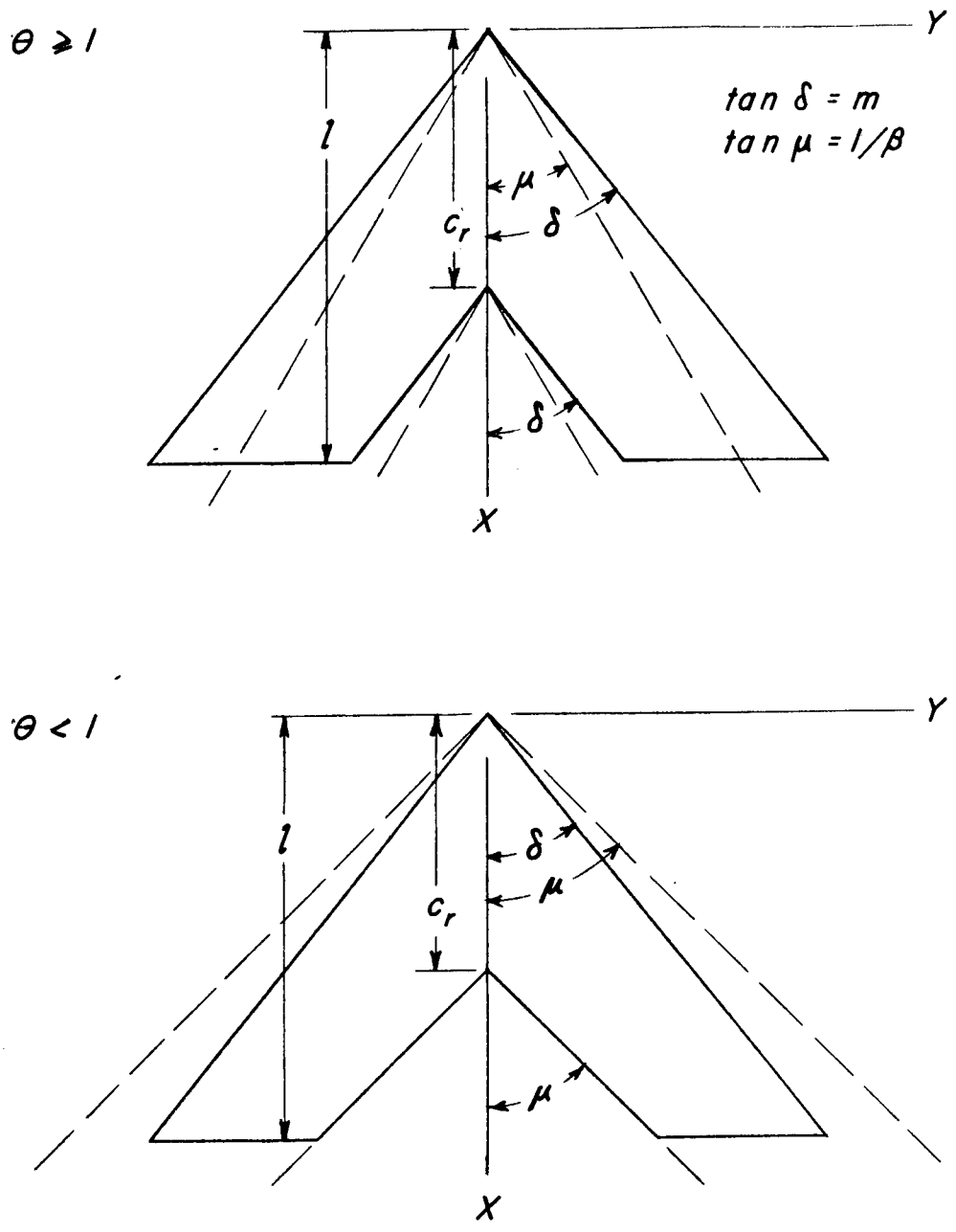

Figure 2.- Swept-back planforms and Mach cone configurations investigated.

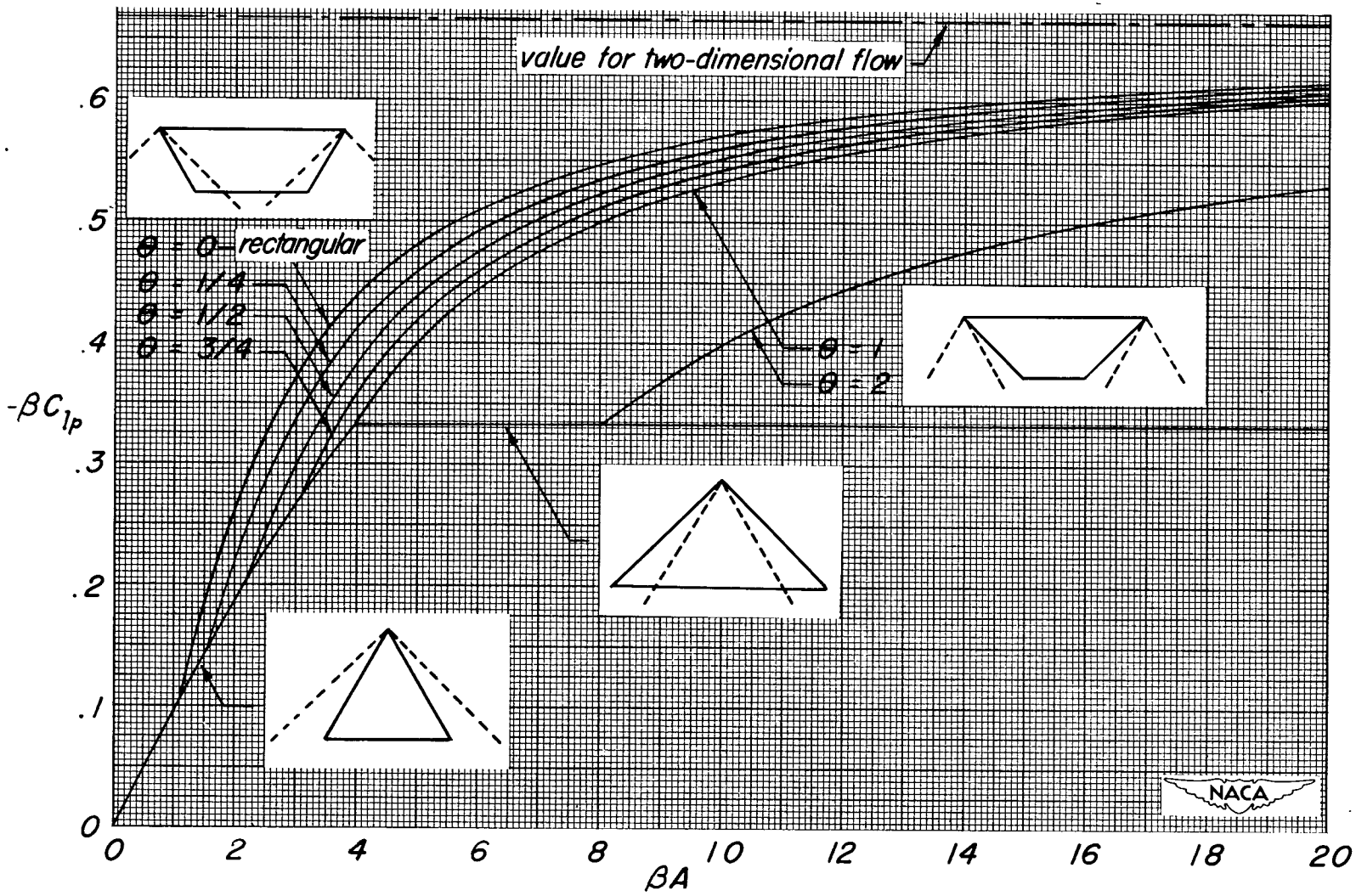

Figure 3.- Variation of damping-in-roll coefficient, βC_{l_p}, with aspect ratio parameter, βA, for trapezoidal and triangular planforms investigated.

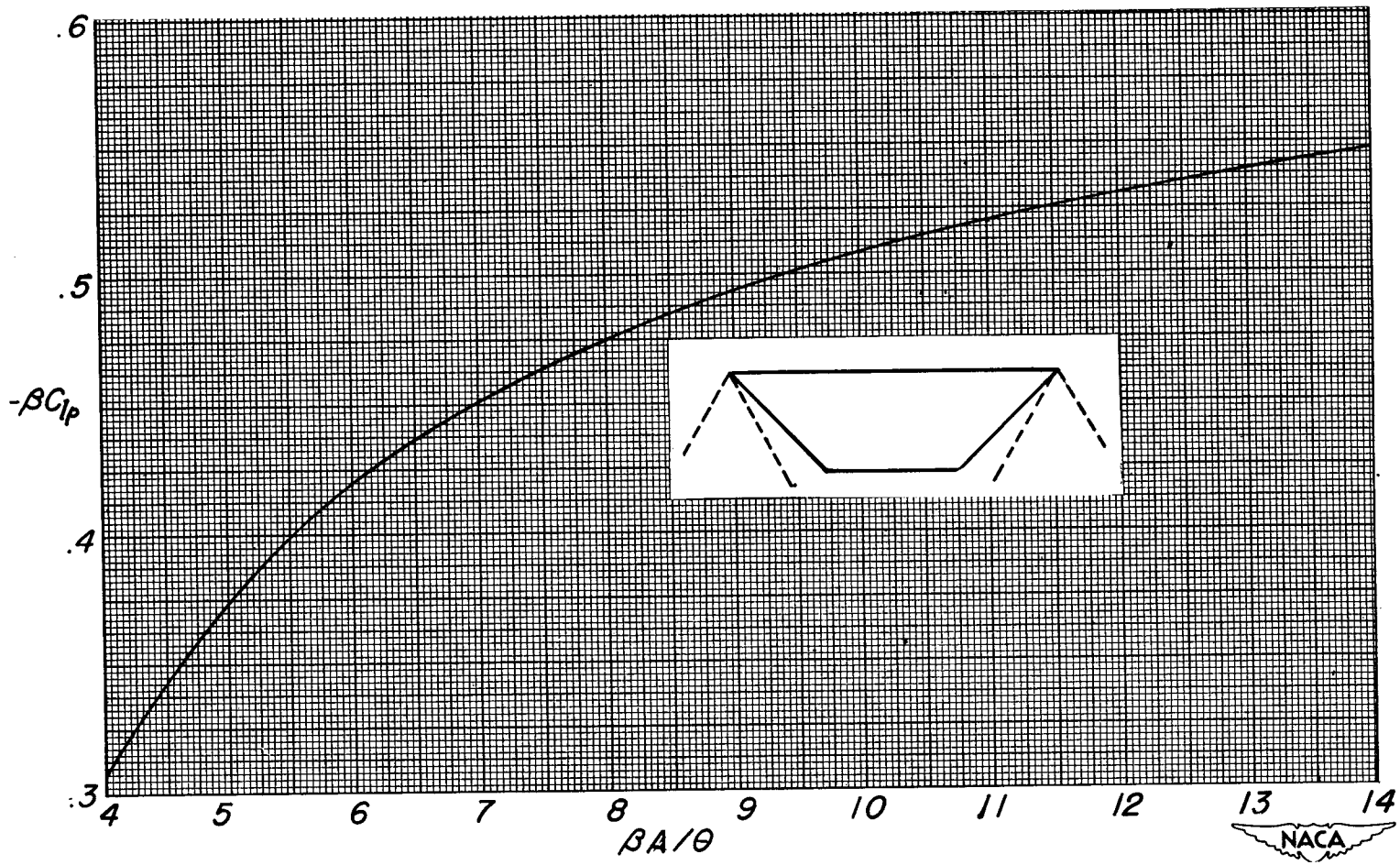

Figure 4. - Variation of damping-in-roll coefficient, βC_{lp}, with aspect ratio parameter, $\beta A/\theta$, for trapezoidal planforms with supersonic tips, $\theta \gg 1$.

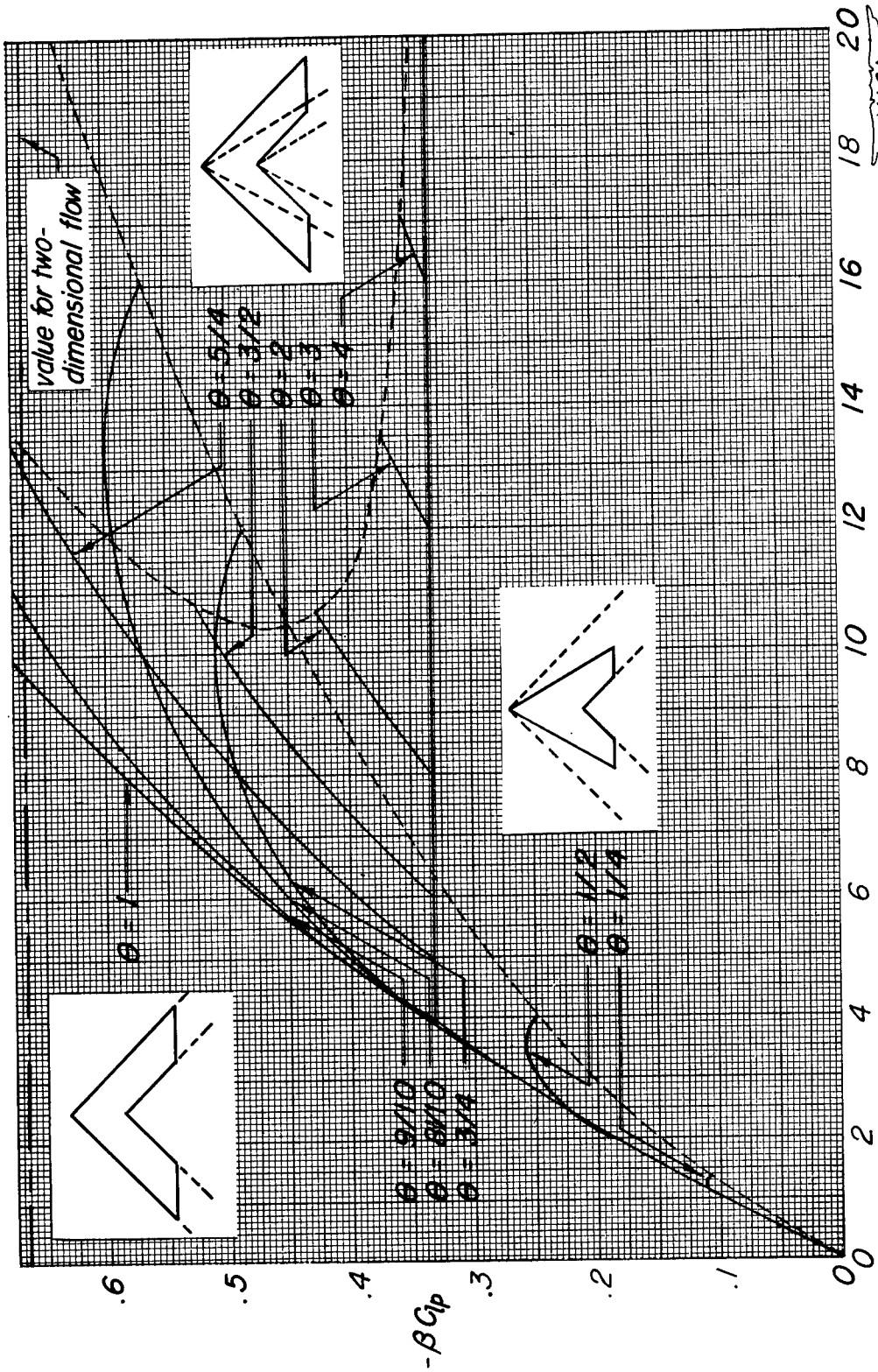

Figure 5.- Variation of damping-in-roll coefficient, βC_{l_p}, with aspect ratio parameter, βA, for swept-back planforms investigated.